remote sensing

Technical Note

A New MODIS C6 Dark Target and Deep Blue Merged Aerosol Product on a 3 km Spatial Grid

Muhammad Bilal [1], Zhongfeng Qiu [1,*], James R. Campbell [2], Scott N. Spak [3], Xiaojing Shen [4] and Majid Nazeer [5]

1 School of Marine Sciences, Nanjing University of Information Science & Technology, Nanjing 210044, China; muhammad.bilal@connect.polyu.hk
2 Naval Research Laboratory, Monterey, CA 93943, USA; james.campbell@nrlmry.navy.mil
3 School of Urban & Regional Planning, University of Iowa, Iowa City, IA 52242, USA; scott-spak@uiowa.edu
4 School of Atmospheric Sciences, Nanjing University of Information Science & Technology, Nanjing 210044, China; ShenXJ@nuist.edu.cn
5 Earth and Atmospheric Remote Sensing Lab (EARL), Department of Meteorology, COMSATS Institute of Information Technology, Islamabad 45550, Pakistan; majid.nazeer@comsats.edu.pk
* Correspondence: zhongfeng.qiu@nuist.edu.cn; Tel.: +86-025-5869-5696

Received: 16 February 2018; Accepted: 13 March 2018; Published: 15 March 2018

Abstract: In Moderate Resolution Imaging Spectroradiometer (MODIS) Collection (C6) aerosol products, the Dark Target (DT) and Deep Blue (DB) algorithms provide aerosol optical depth (AOD) observations at 3 km (DT_{3K}) and 10 km (DT_{10K}), and at 10 km resolution (DB_{10K}), respectively. In this study, the DB_{10K} is resampled to 3 km grid (DB_{3K}) using the nearest neighbor interpolation technique and merged with DT_{3K} to generate a new DT and DB merged aerosol product (DTB_{3K}) on a 3 km grid using Simplified Merge Scheme (SMS). The goal is to supplement DB_{10K} with high-resolution information over dense vegetation regions where DT_{3K} is susceptible to error. SMS is defined as "an average of the DT_{3K} and DB_{3K} AOD retrievals or the available one with the highest quality flag". The DT_{3K} and DTB_{3K} AOD retrievals are validated from 2008 to 2012 against cloud-screened and quality-assured AOD from 19 AERONET sites located in Europe. Results show that the percentage of DTB_{3K} retrievals within the expected error (EE = $\pm$ (0.05 + 20%)) and data counts are increased by 40% and 11%, respectively, and the root mean square error and the mean bias are decreased by 26% and 54%, respectively, compared to the DT_{3K} retrievals. These results suggest that the DTB_{3K} product is a robust improvement over DT_{3K} alone, and can be used operationally for air quality and climate-related studies as a high-resolution supplement to the current MODIS product suite.

Keywords: AERONET; MODIS C6; AOD; DT AOD; DB AOD; Merged AOD

1. Introduction

Atmospheric aerosols, small tiny particles suspended in the atmosphere, are emitted from multiple sources by anthropogenic and natural activities, including smoke, volcanic ash, dust particles, biomass burning, and particular matters. These particles are associated with uncertainties in the Earth's radiation budget and climatic system [1], degradation of atmospheric visibility [2,3], and public health diseases and mortality [4–9]. A ground–based sunphotometer network [10–12] has been established for regular monitoring of aerosol particles by providing high temporal and spectral information, but this network is spatially limited, particularly over open oceans. Satellite remote sensing overcomes this limitation and provides a spatial distribution of aerosol optical properties such as aerosol optical depth (AOD) on the global scale. AOD can be obtained from geostationary and polar satellites at different spatiotemporal resolutions over both land and ocean surfaces [13–26].

The Moderate Resolution Imaging Spectroradiometer (MODIS) sensors onboard the Terra and Aqua satellites provide geophysical observations at 36 channels ranging from 0.4 to 14.4 μm with a temporal resolution of 1–2 days and spatial resolution of 250 m, 500 m, and 1000 m. In the MODIS Collection 5.1 (C5.1) level-2 operational aerosol product, daily AOD observations at 10 km resolution are available over dark surfaces from the Dark Target (DT_{10K}) land algorithm [13,27,28], over ocean surfaces from the DT ocean algorithm [13,29], and over bright surfaces from the Deep Blue (DB_{10K}) algorithm [16,30,31]. These AOD observations are unable to resolve many local-level aerosol features due to their inherently coarse resolution. Therefore, the DT AOD product at 3 km resolution (DT_{3K}) is introduced in the Collection 6 (C6) operational AOD product [32], as a supplement to the DT_{10K} [13] and DB_{10K} [16] AOD products. DT_{3K} is generated using the same inversion method as used in DT_{10K}, the only difference being in the selection of the dark target pixels [32].

For the development of the DT_{3K} algorithm over land [13,32], dark target pixels are selected using the top-of-atmosphere (TOA) reflectance between 0.01 and 0.25 in the 2.11 μm channel. Then, selected pixels are organized into retrieval windows of 6 pixels × 6 pixels (36 pixels) for subsequent aerosol retrievals. Pixels in the retrieval windows are masked for clouds, snow/ice, and other bright surfaces, and separated by land and water pixels. From the remaining pixels, the darkest 20% and brightest 50% in the retrieval window are discarded using the 0.66 μm channel with, at most, 11 pixels in the retrieval window being required to perform aerosol retrievals. In this process, pixels retained at 3 km resolution might be discarded at 10 km resolution. With fewer pixels contributing to the DT_{3K} retrieval, it yields a noisier product than the DT_{10K} retrieval [13,32]. The DT_{3K} product has been validated over several regions and exhibits larger errors than the DT_{10K} product due to underestimation of the estimated surface reflectance and incorrect use of the available "look-up" aerosol models [13,32–36]. The expected error (EE) of the DT_{3K} over land is ±(0.05 + 20%) [13,32] which represents a one standard deviation confidence interval around the retrieved AOD (i.e., about 68% of points should fall within ±EE from the true AOD).

Initially, the MODIS DB algorithm was developed to retrieve AOD over bright surfaces [30,31]. In C6, the Enhanced DB algorithm is used to retrieve AOD over both bright as well as dark surfaces [16,37,38]. In developing the DB algorithm, pixels are masked for clouds and snow/ice surfaces, and surface reflectance is estimated for the remaining pixels at 0.412, 0.47, and 0.65 μm. Thus, AOD is retrieved at 1 km resolution by finding the best match between satellite TOA reflectance and pre-calculated TOA reflectance stored in a look-up-table (LUT), and then all available pixels are aggregated at 10 km resolution. The DB_{10K} AOD product has been validated in previous studies, which have reported better relative retrieval accuracy than the DT_{10K} AOD product [35,38–40] with some exceptions [41]. EE for Deep Blue is dependent on the viewing geometry, but is approximately 0.03 + 20% on average (i.e., the algorithms have different error characteristics).

MODIS-retrieved AOD [13,16,42–46] is the most frequently used parameter for mapping and estimation of fine particulate matter ($PM_{2.5}$) from local to global scales. The error in MODIS AOD may cause under-/over-estimation in $PM_{2.5}$ concentrations. Therefore, quality assessment of MODIS AOD is crucial for local and global air quality applications. Studies have performed the quality assessment of the MODIS AOD [35,36,41,42,47–50] and used it in statistical modeling based on the empirical linear regression, land use regression model, and Geo-graphically Weighted Regression (GWR) model for estimation of $PM_{2.5}$ concentrations at regional and global scales [14,51–64]. These studies found that an accurate estimation of the $PM_{2.5}$ concentration depends on the quality of the satellite-retrieved AOD observations. Therefore, accurate and robust satellite retrieved AOD retrievals are much needed for solving environmental and air pollution problems.

Previous studies [33,34,36,40] have reported large uncertainty in the DT_{3K} AOD product at local-to-regional scales. For example, Nichol and Bilal [36] validated the DT_{3K} AOD retrievals over 16 AERONET sites in Asia corresponding with urban and vegetated land surfaces, and they found larger errors and overestimation in DT_{3K}. In addition, the DT and DB algorithms have different AOD spatial coverages over land due to differences in pixels selection criteria and their thresholds, the surface reflectance calculation method, and cloud mask. Therefore, a new product at higher resolution with low errors and more spatial coverage is preferable to understanding aerosol behavior at something approaching the level of an urban city center.

The main objective of this study is to describe and evaluate a new DT and DB-merged (DTB_{3K}) AOD product on a 3 km grid to improve the quality of AOD retrievals and spatial coverage over vegetated and non-vegetated land surfaces (i.e., to retrieve AOD for those regions where the DT_{3K} does not retrieve AOD due to pixels selection criteria and cloud mask [13], and where DB_{10K} does not retrieve AOD due to errors in cloud mask that lead to removal of cloud free pixels [16,37]). This study validates DT_{3K} and DTB_{3K} AOD products over European AERONET sites located over vegetated surfaces, as the AOD product at 3 km resolution is only available for the DT algorithm which is supposed to retrieve AOD accurately over vegetated surfaces. However, the proposed product can be used over other global non-vegetated land surfaces since the product will weigh considerably more information from the DB algorithm which is designed to retrieve AOD accurately over non-vegetated surfaces. To support this hypothesis, one urban AERONET is also included in the validation experiment. Dataset and methods are described in Sections 2 and 3, respectively, and Sections 4 and 5 are about results and discussion, and conclusion, respectively.

2. Dataset

In this study, Terra–MODIS C6 level-2 operational aerosol products at 3 km (MOD04_3K) and 10 km (MOD04) spatial resolutions were downloaded from Level-1 and Atmosphere Archive & Distribution System (LAADS) Distributed Active Archive Center (DAAC) (https://ladsweb.nascom.nasa.gov/) to obtain DT_{3K} and DB_{10K} AOD retrievals, respectively, for evaluation and development of the proposed merged 3 km DT and DB aerosol product (DTB_{3K}). The Terra–MODIS monthly level 3 Normalized Difference Vegetation Index (NDVI) product (MOD13A3) was downloaded to obtain the parameter "1 km NDVI" to derive average NDVI values for each corresponding validation site (Table 1). Aerosol Robotic Network (AERONET) [10,11] cloud-screened and quality-assured (Level 2.0 Version 2) AOD data [12] were downloaded from http://aeronet.gsfc.nasa.gov for 19 European sites from 2008 to 2012.

Table 1. Summary of the AERONET sites used in this study from 2008 to 2012.

Site	Latitude (°N)	Longitude (°E)	Elevation (m)	Avg. NDVI	Country
Aubiere LAMP	45.76096	3.11107	423.0	0.36	France
Avignon	43.93275	4.87807	32.0	0.54	France
Brussels	50.78333	4.35000	120.0	0.59	Belgium
Cabauw	51.97100	4.92700	−0.7	0.72	Netherlands
Carpentras	44.08333	5.05833	100.0	0.45	France
Chilbolton	51.14446	1.43698	88.0	0.60	UK
Hamburg	53.56833	9.97333	105.0	0.37	Germany
Ispra	45.80305	8.62670	235.0	0.57	Italy
Kanzelhohe Obs.	46.67800	13.90700	1526.0	0.65	Austria
Leipzig	51.35250	12.43528	125.0	0.44	Germany
Lille	50.61167	3.14167	60.0	0.45	France
Minsk	53.92000	27.60100	200.0	0.32	Belarus
Moscow MSU MO	55.70000	37.51000	192.0	0.31	Russia
Munich University	48.14800	11.57300	533.0	0.37	Germany
OHP OBSERVATOIRE	43.93500	5.71000	680.0	0.55	France
Palaiseau	48.70000	2.20833	156.0	0.57	France
Paris	48.86667	2.33333	50.0	0.15	France
Rome Tor Vergata	41.83955	12.64733	130.0	0.48	Italy
Toravere	58.25500	26.46000	70.0	0.50	Estonia

3. Methods

DT_{3K} and merged DTB_{3K} AOD retrievals were validated from 2008 to 2012 against the 19 European AERONET sites. As the MODIS DT algorithm is designed to retrieve AOD over vegetated surfaces (NDVI > 0.3) [13], the AERONET sites selected for validation correspond with adjacent surfaces exhibiting NDVI values between 0.31 and 0.75, except one (Paris) with NDVI of 0.15 that is an urban site (Table 1). The methodology of this study is based on the following steps:

(i) Only those DT_{3K} and DB_{10K} AOD retrievals at 0.55 µm passing recommended quality assurance (AQ) checks [13,16,37] were used (for DT, this corresponds to retrievals flagged QA = 3, and, for DB, retrievals flagged QA = 2 or QA = 3). Therefore, the DT_{3K} and DB_{10K} highest-quality retrievals were obtained from the Scientific Data Set (SDS) "Optical_Depth_Land_And_Ocean" and "Deep_Blue_Aerosol_Optical_Depth_550_Land_Best_Estimate", respectively.

(ii) DB_{10K} AOD retrievals were resampled to 3 km spatial grid (DB_{3k}) onto the DT_{3K} grid using the nearest neighbor interpolation algorithm [65,66] to match and overlap pixels of DB_{3K} with the pixels of DT_{3K}. As the DB algorithm first retrieves AOD at 1 km resolution, by finding the best match between satellite TOA reflectance and pre-calculated TOA reflectance stored in a LUT, all available pixels are then aggregated to 10 km resolution [16,37,38]. It is expected that resampling from 10 to 3 km will not affect the accuracy and quality of the DB AOD retrievals.

(iii) To reduce errors in DT_{3K}, the DTB_{3k} product is generated using the Simplified Merge Scheme (SMS) (DTB_{M1} in [39]). This technique is selected as it increases the number of collocations and decreases the errors, and is defined as "an average of the DT_{3K} and DB_{3K} AOD retrievals or the available one with highest quality assurance flag" independent of the NDVI values [39]. This proposed technique differs from the operational DTB_{10K} technique [13], which uses "an average of the DT_{10K} and DB_{10K} AOD retrievals or available one for only 0.2 < NDVI < 0.3". Instead, the proposed technique uses "an average the DT_{10K} and DB_{10K} AOD retrievals or available one" for all available NDVI values.

(iv) AERONET AOD is interpolated to 0.55 µm using a standard Ångström exponent (α) extrapolation [37], as the project does not provide AOD measurements directly at this common MODIS wavelength.

(v) To increase the number of samples for validation, collocations are defined as the average of at least two AERONET AOD measurements between 10:00 and 12:00 local solar time and at least two pixels of MODIS AOD observations within a sampling window of 3 pixels × 3 pixels (average of 9 pixels) centered on the AERONET site. (i.e., an average within a 9 km × 9 km region).

(vi) Retrieval errors are reported using the expected error (EE) of the *DT* algorithm at 3 km resolution over land [32], root mean square error (RMSE), and mean bias (MB). To compare DT_{3K} and DTB_{3K} statistically, the percent relative differences in N, EE Equation (1), RMSE Equation (2), MB Equation (3), and R Equation (4) are calculated using Equation (5). These relationships are defined as

$$\mathrm{EE} = \pm\left(0.05 + 0.20 \times AOD_{(AERONET)}\right) \tag{1}$$

$$\mathrm{RMSE} = \sqrt{\frac{1}{n}\sum_{i=1}^{n}\left(AOD_{(MODIS)i} - AOD_{(AERONET)i}\right)^2} \tag{2}$$

$$\mathrm{MB} = \overline{AOD}_{(MODIS)} - \overline{AOD}_{(AERONET)} \tag{3}$$

$$\mathrm{R} = \frac{n\sum AERONET_i \times MODIS_i - \sum AERONET_i \times \sum MODIS_i}{\sqrt{\left[n\sum(AERONET_i)^2 - \left(\sum AERONET_i\right)^2\right] \times \left[n\sum(MODIS_i)^2 - \left(\sum MODIS_i\right)^2\right]}} \tag{4}$$

and

$$\%\ Relative\ Difference = \left(\frac{DT_{3K} - DTB_{3K}}{DT_{3K}}\right) \times 100 \tag{5}$$

4. Results and Discussion

4.1. Validation of the DT_{3K} and DTB_{3K} AOD Products at Regional Scale

DT_{3K} and DTB_{3K} AOD retrievals were validated from 2008 to 2012 (Figure 1 and Table 2) against AERONET. In Figure 1, red and black colors represent the coincident DT_{3K} and DTB_{3K} observations, respectively (dashed lines = EE envelopes, and the black solid line = 1:1 line). Figure 1 shows that the DT_{3K} AOD retrievals, in general, overestimate at all of the sites, although large variance was observed between them overall. This overestimation of AOD retrievals by DT_{3K} was observed at 13 out of 19 sites, while AOD retrievals at only six sites meet the requirement of the *EE* (>68% or 69% to 88% of the retrievals were within the *EE*). The greatest uncertainties were observed at Paris (NDVI = 0.15), Moscow_MU_MO (NDVI = 0.31), Leipzig (NDVI = 0.44), and Minsk (NDVI = 0.32), with only 8%, 14%, 26% and 27% of the retrievals, respectively, being within *EE* (Figure 1 and Table 2). This overestimation, occurring for both low and high aerosol loadings, probably implies an underestimation of the surface reflectance by the VIS vs. 2.11 µm relationship, and potentially an error in the aerosol schemes used in the LUT. Previous studies reported similar errors in the DT_{3K} AOD retrievals over different parts of the globe [32–34,36]. This is also similar to the DT C6 algorithm at 10 km, which overestimates with positive offset [34–36,67,68].

Table 2. Validation summary of the DT_{3K} and DTB_{3K} AOD retrievals.

Site	N	% Above/Within/Below EE	RMSE	MB	R
		DT_{3K} AOD Product			
Aubiere LAMP	232	40/60/00	0.116	0.073	0.731
Avignon	783	34/66/00	0.092	0.064	0.853
Brussels	211	33/67/00	0.104	0.063	0.817
Cabauw	219	19/78/03	0.093	0.040	0.837
Carpentras	258	31/69/00	0.078	0.057	0.861
Chilbolton	241	24/75/01	0.101	0.041	0.728
Hamburg	149	66/34/00	0.154	0.127	0.835
Ispra	183	09/88/03	0.078	0.012	0.913
Kanzelhohe Obs.	96	43/53/00	0.092	0.067	0.623
Leipzig	293	74/26/00	0.164	0.137	0.832
Lille	303	58/40/02	0.139	0.107	0.793
Minsk	161	73/27/00	0.163	0.135	0.828
Moscow MSU MO	173	86/14/00	0.200	0.179	0.888
Munich University	257	59/40/01	0.128	0.104	0.794
OHP OBSERVATOIRE	765	24/76/00	0.070	0.045	0.834
Palaiseau	354	38/61/01	0.102	0.066	0.787
Paris	212	92/08/00	0.362	0.311	0.533
Rome Tor Vergata	675	54/45/01	0.122	0.096	0.778
Toravere	261	25/74/01	0.098	0.053	0.811
All sites	5826	43/56/01	0.131	0.085	0.769
		DTB_{3K} AOD Product			
Aubiere LAMP	240	20/79/01	0.100	0.043	0.724
Avignon	897	15/84/01	0.068	0.023	0.809
Brussels	223	23/77/00	0.095	0.048	0.802
Cabauw	266	14/82/04	0.088	0.019	0.817
Carpentras	268	20/80/00	0.067	0.037	0.828
Chilbolton	254	15/83/02	0.095	0.022	0.717
Hamburg	188	19/80/01	0.094	0.036	0.804
Ispra	276	04/85/11	0.076	−0.019	0.897
Kanzelhohe Obs.	120	24/73/03	0.084	0.027	0.552
Leipzig	324	24/74/02	0.120	0.063	0.760
Lille	325	31/68/01	0.107	0.063	0.787
Minsk	178	34/65/01	0.122	0.066	0.767

Table 2. *Cont.*

Site	N	% Above/Within/Below EE	RMSE	MB	R
		DT_{3K} AOD Product			
Moscow MSU MO	202	30/68/02	0.151	0.072	0.932
Munich University	286	19/79/02	0.082	0.022	0.768
OHP OBSERVATOIRE	779	17/83/00	0.062	0.030	0.803
Palaiseau	369	18/79/03	0.083	0.025	0.751
Paris	304	34/63/03	0.188	0.083	0.495
Rome Tor Vergata	717	28/71/01	0.097	0.052	0.734
Toravere	276	26/73/01	0.094	0.051	0.802
All sites	6492	21/77/02	0.097	0.039	0.801

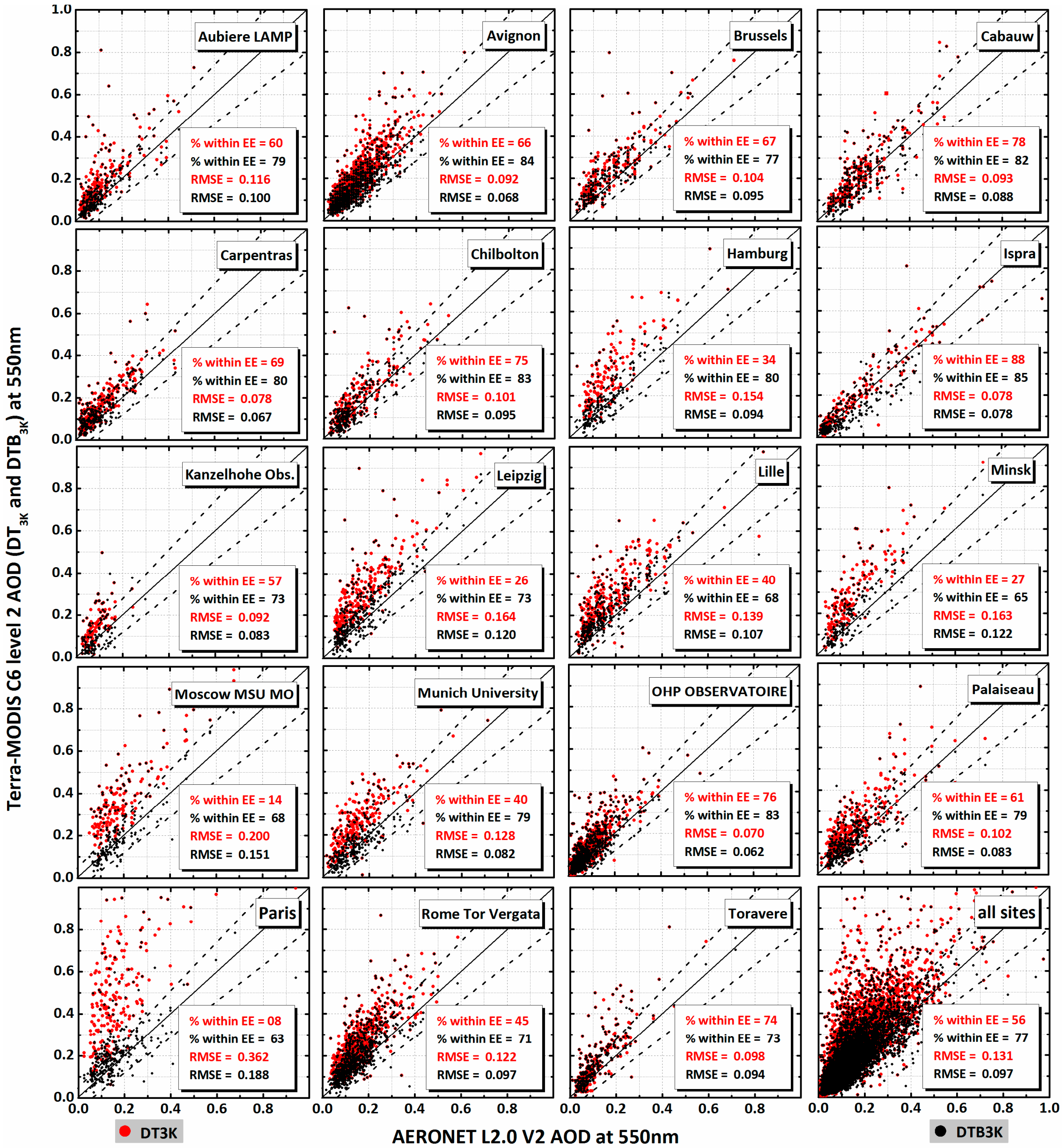

Figure 1. Validation of DT_{3K} and DTB_{3K} AOD products against 19 AERONET sites located at vegetated surfaces (NDVI > 0.30), except Paris (NDVI < 0.20), from 2008 to 2012.

The aggregated results of all sites show a large and significant overestimation in the DT_{3K} AOD retrievals, as 43% of the retrievals were above *EE* (Table 2). All these sites have different surface characteristics. For example, Paris is a pure urban site, whereas Leipzig is dominated by vegetated surfaces. For Paris and Leipzig, the slope between DT_{3K} and AERONET was significantly greater than one (Paris = 1.99 and Leipzig = 1.47), which probably suggests too much absorption in the aerosol model used in the LUT [38,69]. However, both generally experience a wide range of aerosol loading conditions. Thus, selection of an accurate aerosol model is important for accurate high AOD retrievals [13]. Overall, the performance of DT_{3K} was relatively poor over the vegetated surfaces (NDVI > 0.30), as only 56% of the retrievals were within EE with RMSE of 0.131 and MB of 0.085. This is an important distinction, though, as the point of designing the retrieval was ultimately more accurate AOD over such surfaces.

Validation of the DTB_{3K} AOD retrievals show significant improvement in retrieval quality, as the percentage of retrievals within EE increased and RMSE and MB decreased at each site (Figure 1 and Table 2). For the Paris, Moscow_MU_MO, Leipzig, and Minsk sites, for instance, the percentage of retrievals within EE increased remarkably from 8% to 63%, 14% to 68%, 26% to 73%, and 27% to 65%, respectively; RMSE decreased from 0.362 to 0.188, 0.200 to 0.151, 0.164 to 0.120, and 0.163 to 0.122, respectively; and MB decreased from 0.311 to 0.083, 0.179 to 0.072, 0.137 to 0.063, and 0.135 to 0.066 (Table 2), respectively. These results suggest that the DB algorithm performs better at these sites compared with DT and the contribution of the DB AOD retrievals in the DTB_{3K} retrievals significantly improves the retrieval quality and reduces error. Again, the advantage of using the average of both DT and DB AOD retrievals is to minimize the error in the DT C6 algorithm [39].

For all sites, 77% of the DTB_{3K} AOD retrievals were within EE, which is 38% higher than the DT_{3K} AOD retrievals, RMSE and MB decreased from 0.131 to 0.097 and 0.087 to 0.039, which are 26% and 54%, respectively, lower than the DT_{3K}. These results suggest that a merged DTB_{3K} AOD product exhibits better retrieval quality than the DT_{3K} and can thus be applied with greater confidence for air quality studies at the relatively finer scales.

4.2. Validation of the DT_{3K} and DTB_{3K} AOD Products at Local Scales

The performance of the DT_{3K} and DTB_{3K} AOD products was further evaluated in terms of improvement in percentage of retrievals within EE, spatiotemporal data coverage, RMSE and MB and R at each AERONET site based on the following criteria [39]: if the relative difference using Equation (5) is (a) within 10% for the percentage of retrievals within EE; (b) within 20% for the data count (N); (c) within 5% for RMSE; (d) within 5% for MB; and (e) within 10% for R, then the DT_{3K} and DTB_{3K} are considered to perform equally well at that site, and these sites are denoted by a "plus" symbol in Figure 2. In Figure 2, DT_{3K} and DTB_{3K} are represented by "triangle" and "circle" symbols, respectively, when they performed better over the individual sites, and color variations represent the magnitude of the relative difference (%) between the DT_{3K} and DTB_{3K} AOD products. The point of this analysis is to highlight the robustness of the AOD product with respect to each statistical parameter for each individual site.

For the percentage of AOD retrievals within EE, the DTB_{3K} AOD product performed well, as 15 out of 19 sites showed improvement and the percentage of AOD retrievals within EE was increased by 11% to >100% compared with the DT_{3K} AOD product (Figure 2a). There were only four sites where DT_{3K} and DTB_{3K} performed equally, as the relative difference of the percentage of retrievals within EE is less than 10%. Overall, the DTB_{3K} method performed well and significantly improved retrieval quality, as the percentage of AOD retrievals within EE increased due to the contribution of the DB AOD retrievals.

For the data count, or number of collocations, the DT_{3K} and DTB_{3K} methods performed equally at 14 out of 19 sites, as the relative difference of data counts is within 20% (Figure 2b). For the remaining five sites, DTB_{3K} performed well compared with DT_{3K} as the data count increased by 21%

to 60%. This indicates that the DTB_{3K} method is likely more skillful than the DT_{3K} method in terms of spatiotemporal data coverage.

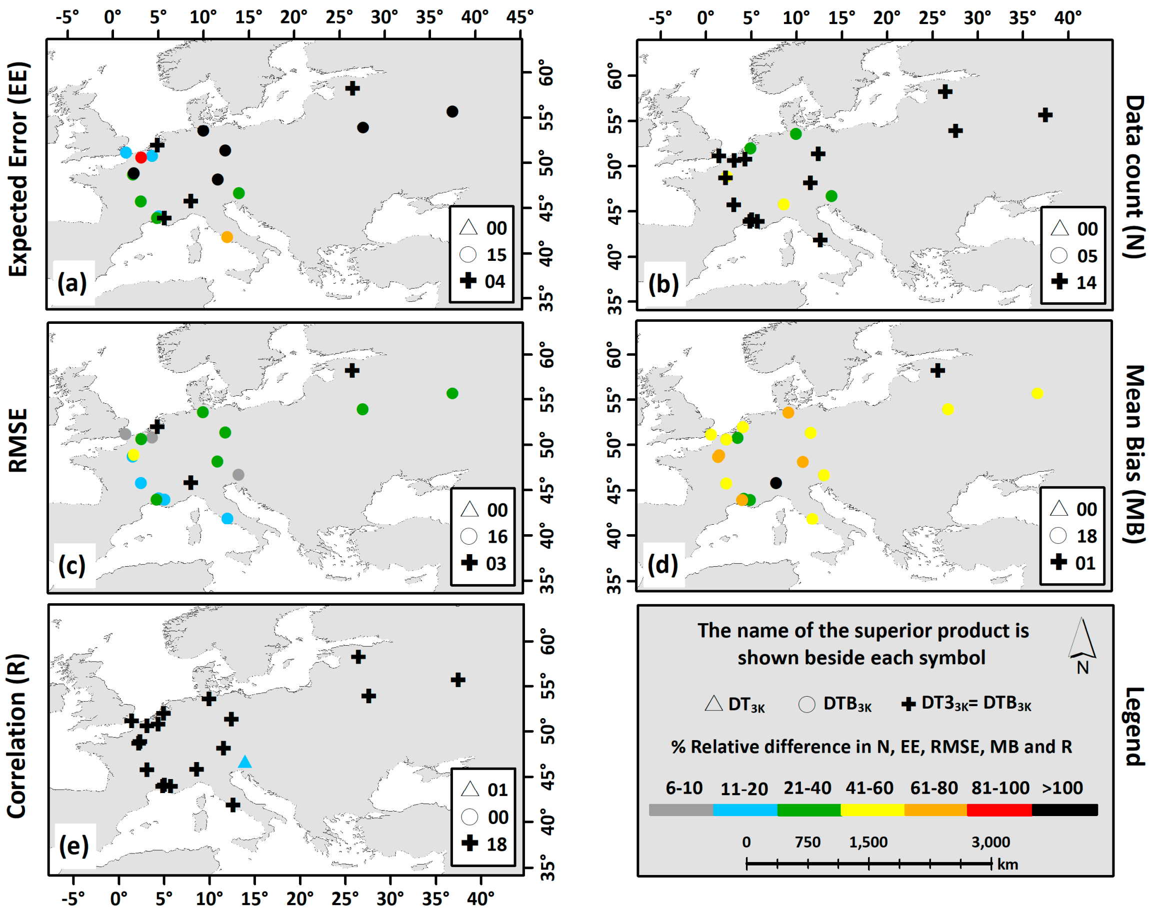

Figure 2. Maps showing the best performing retrieval at AERONET sites for the following evaluation statistics: (**a**) percentage within the EE; (**b**) data count (N); (**c**) root mean square error (RMSE); (**d**) mean bias (MB); and (**e**) correlation coefficient (R).

For RMSE and *MB*, the DTB_{3K} method significantly reduced the errors at 16 (Figure 2c) and 18 (Figure 2d) sites, respectively, compared with DT_{3K}. The RMSE and MB reduced by 6 to 60% and 21 to >100%, respectively. There were only three (one) sites where both methods exhibit the same RMSE (MB). These results suggest that DTB_{3K} is robust, with lower RMSE and MB errors than the DT_{3K} retrievals.

For correlation, the DT_{3K} and DTB_{3K} methods performed equally at 18 out of 19 sites, as the relative difference was within 10% (Figure 2e). There was only one site where the DT_{3K} AOD retrievals have a better correlation with the AERONET AOD retrievals than the DTB_{3K} AOD retrievals as the relative difference was between 11% and 20%. Overall, both methods performed equally in terms of correlation.

In full, these results suggest that the DTB_{3K} method is robust, more efficient and performed better at relatively finer scales, with larger data count percentages within EE, greater data counts overall, and lower RMSE and MB than DT_{3K}.

5. Summary and Conclusions

The Moderate Resolution Imaging Spectroradiometer (MODIS) Collection 6 aerosol product provides global aerosol optical depth (AOD) observations over land at 3 km and 10 km spatial resolutions based on the Dark Target (DT) algorithms, and at 10 km resolution based on the Deep Blue (DB) algorithm. The DT and DB algorithms have different spatial coverage of AOD observations over land due to differences in their retrieval approaches (i.e. pixel selection, cloud screening and surface reflectance estimation method). DT_{3K} exhibits large errors over urban or non-vegetated surfaces, as the DT algorithm is designed to retrieve AOD over vegetated surfaces. Therefore, the objectives of this study included developing a new DT and DB merged aerosol product on a 3 km grid, which can reduce the errors and increase the spatiotemporal coverage by providing AOD observations for those surface types and regions where either of each (DT and DB) were unable to provide due to pixel selection criteria and cloud mask.

For this analysis: (i) only high quality-assured AOD observations were obtained from the Scientific Data Sets (SDS), including "Optical_Depth_Land_And_Ocean" and "Deep_Blue_Aerosol_Optical_Depth_550_Land_Best_Estimate" for DT_{3K} and DB_{10K}, respectively; (ii) the DB_{10K} AOD retrievals were resampled to 3 km grid using nearest neighbor interpolation algorithm; and (iii) they were merged with DT_{3K} AOD retrievals using Simplified Merge Scheme (SMS) defined as "an average of the DT_{3K} and DB_{3K} AOD retrievals or the available one with highest quality assurance flag". DT_{3K} and DTB_{3K} AOD retrievals were validated from 2008 to 2012 against cloud-screened and quality-assured (Level 2.0 Version 2) AOD measurements obtained from the 19 AERONET sites in Europe located over the vegetated and non-vegetated surfaces.

Our primary conclusions are:

(i) DT_{3K} AOD retrievals were overestimated over vegetated surfaces for both low and high aerosol loadings.
(ii) The overestimation might be caused by the underestimation of the surface reflectance and inappropriate aerosol model.
(iii) Only 56% retrievals of the DT_{3K} were within the EE which indicates that the DT_{3K} product does not meet the requirements of the EE.
(iv) The DTB_{3K} method significantly improved the retrieval quality as the percentage of the retrievals and data counts were increased, and RMSE and MB were decreased.
(v) The contribution of DB AOD retrievals in the DTB_{3K} helped to reduce the overestimation in the DT_{3K} AOD retrievals for both low and high aerosol loadings.
(vi) The percentage within the EE for the DTB_{3K} retrievals increased up to 77% which indicates that the DTB_{3K} product meets the requirements of the EE, and this is a 38% relative increase over the DT_{3K} AOD retrievals.
(vii) The DBT_{3K} method reduced the RMSE and MB errors by 26% and 54%, respectively, for all sites.

Overall, the DTB_{3K} merged method is robust and performed better over vegetated and non-vegetated land surfaces than the DT_{3K} algorithm, and is recommended for air quality and climate-related studies in such land–surface regions.

Acknowledgments: The authors acknowledge NASA Goddard Space Flight Center for MODIS data, and Principal Investigators of AERONET sites. We are thankful to Devin White (Oak Ridge National Laboratory) for MODIS Conversion Tool Kit (MCTK). The National Key Research and Development Program of China (No. 2016YFC1400901), the National Programme on Global Change and Air-sea Interaction (GASI-03-03-01-01) and National Science Foundation of China (NSFC) (Project No. 41374013) have sponsored this research.

Author Contributions: Muhammad Bilal designed and wrote the paper; Zhongfeng Qiu, James R. Campbell, and Scott N. Spak reviewed and modified the paper; and Shen Xiaojing and Majid Nazeer helped in data processing.

Conflicts of Interest: The authors declare no conflict of interest.

References

1. Kaufman, Y.J.; Tanré, D.; Boucher, O. A satellite view of aerosols in the climate system. *Nature* **2002**, *419*, 215–223. [CrossRef] [PubMed]
2. Cheung, H.-C.; Wang, T.; Baumann, K.; Guo, H. Influence of regional pollution outflow on the concentrations of fine particulate matter and visibility in the coastal area of southern China. *Atmos. Environ.* **2005**, *39*, 6463–6474. [CrossRef]
3. Park, R.J.; Jacob, D.J.; Kumar, N.; Yantosca, R.M. Regional visibility statistics in the United States: Natural and transboundary pollution influences, and implications for the Regional Haze Rule. *Atmos. Environ.* **2006**, *40*, 5405–5423. [CrossRef]
4. Bell, M.L.; Ebisu, K.; Belanger, K. Ambient air pollution and low birth weight in Connecticut and Massachusetts. *Environ. Health Perspect.* **2007**, *115*, 1118–1124. [CrossRef] [PubMed]
5. Dominici, F.; Peng, R.D.; Bell, M.L.; Pham, L.; McDermott, A.; Zeger, S.L.; Samet, J.M. Fine particulate air pollution and hospital admission for cardiovascular and respiratory diseases. *JAMA* **2006**, *295*, 1127–1134. [CrossRef] [PubMed]
6. Götschi, T.; Heinrich, J.; Sunyer, J.; Künzli, N. Long-term effects of ambient air pollution on lung function: A review. *Epidemiology* **2008**, *19*, 690–701. [CrossRef] [PubMed]
7. Pope, C.A.; Burnett, R.T.; Thun, M.J.; Calle, E.E.; Krewski, D.; Ito, K.; Thurston, G.D. Lung cancer, cardiopulmonary mortality, and long-term exposure to fine particulate air pollution. *JAMA* **2002**, *287*, 1132–1141. [CrossRef] [PubMed]
8. Pope, C.A.; Dockery, D.W. Health effects of fine particulate air pollution: Lines that connect. *J. Air Waste Manag. Assoc.* **2006**, *56*, 709–742. [CrossRef]
9. Pope, C.A.; Ezzati, M.; Dockery, D.W. Fine-particulate air pollution and life expectancy in the United States. *N. Engl. J. Med.* **2009**, *360*, 376–386. [CrossRef] [PubMed]
10. Holben, B.N.; Eck, T.F.; Slutsker, I.; Tanré, D.; Buis, J.P.; Setzer, A.; Vermote, E.; Reagan, J.A.; Kaufman, Y.J.; Nakajima, T.; et al. Aeronet—A federated instrument network and data archive for aerosol characterization. *Remote Sens. Environ.* **1998**, *66*, 1–16. [CrossRef]
11. Holben, N.; Tanr, D.; Smirnov, A.; Eck, T.F.; Slutsker, I.; Newcomb, W.W.; Schafer, J.S.; Chatenet, B.; Lavenu, F.; Kaufman, J.; et al. An emerging ground-based aerosol climatology: Aerosol optical depth from AERONET . *J. Geophys. Res. Atmos.* **2001**, *106*, 12067–12097. [CrossRef]
12. Smirnov, A.; Holben, B.N.; Eck, T.F.; Dubovik, O.; Slutsker, I. Cloud-screening and quality control algorithms for the AERONET database. *Remote Sens. Environ.* **2000**, *73*, 337–349. [CrossRef]
13. Levy, R.C.; Mattoo, S.; Munchak, L.A.; Remer, L.A.; Sayer, A.M.; Patadia, F.; Hsu, N.C. The Collection 6 MODIS aerosol products over land and ocean. *Atmos. Meas. Tech.* **2013**, *6*, 2989–3034. [CrossRef]
14. Aaron, V.D.; Randall, V.M.; Robert, J.D.S.; Richard, T.B. High-resolution satellite-derived PM2.5 from optimal estimation and geographically weighted regression over North America. *Environ. Sci. Technol.* **2015**, *49*, 10482–10491.
15. Hauser, A.; Oesch, D.; Foppa, N.; Wunderle, S. NOAA AVHRR derived aerosol optical depth over land. *J. Geophys. Res.* **2005**, *110*, D08204. [CrossRef]
16. Hsu, N.C.; Jeong, M.-J.; Bettenhausen, C.; Sayer, A.M.; Hansell, R.; Seftor, C.S.; Huang, J.; Tsay, S.-C. Enhanced deep blue aerosol retrieval algorithm: The second generation. *J. Geophys. Res. Atmos.* **2013**, *118*, 9296–9315. [CrossRef]
17. Jackson, J.M.; Liu, H.; Laszlo, I.; Kondragunta, S.; Remer, L.A.; Huang, J.; Huang, H.-C. Suomi-NPP VIIRS aerosol algorithms and data products. *J. Geophys. Res. Atmos.* **2013**, *118*, 12673–12689. [CrossRef]
18. Kahn, R.A.; Gaitley, B.J.; Garay, M.J.; Diner, D.J.; Eck, T.F.; Smirnov, A.; Holben, B.N. Multiangle imaging spectroradiometer global aerosol product assessment by comparison with the aerosol robotic network. *J. Geophys. Res.* **2010**, *115*, D23209. [CrossRef]
19. Kahn, R.A.; Gaitley, B.J.; Martonchik, J.V.; Diner, D.J.; Crean, K.A.; Holben, B. Multiangle Imaging Spectroradiometer (MISR) global aerosol optical depth validation based on 2 years of coincident Aerosol Robotic Network (AERONET) observations. *J. Geophys. Res.* **2005**, *110*, D10S04. [CrossRef]
20. Liu, H.; Remer, L.A.; Huang, J.; Huang, H.-C.; Kondragunta, S.; Laszlo, I.; Oo, M.; Jackson, J.M. Preliminary evaluation of S-NPP VIIRS aerosol optical thickness. *J. Geophys. Res. Atmos.* **2014**, *119*, 3942–3962. [CrossRef]

21. Remer, L.a.; Kaufman, Y.J.; Tanré, D.; Mattoo, S.; Chu, D.a.; Martins, J.V.; Li, R.-R.; Ichoku, C.; Levy, R.C.; Kleidman, R.G.; et al. The MODIS aerosol algorithm, products, and validation. *J. Atmos. Sci.* **2005**, *62*, 947–973. [CrossRef]
22. Riffler, M.; Popp, C.; Hauser, A.; Fontana, F.; Wunderle, S. Validation of a modified avhrr aerosol optical depth retrieval algorithm over central europe. *Atmos. Meas. Tech.* **2010**, *3*, 1255–1270. [CrossRef]
23. Sayer, A.M.; Hsu, N.C.; Bettenhausen, C.; Jeong, M.-J.; Holben, B.N.; Zhang, J. Global and regional evaluation of over-land spectral aerosol optical depth retrievals from SeaWiFS. *Atmos. Meas. Tech.* **2012**, *5*, 1761–1778. [CrossRef]
24. Torres, O.; Bhartia, P.K.; Herman, J.R.; Sinyuk, A.; Ginoux, P.; Holben, B. A long-term record of aerosol optical depth from toms observations and comparison to AERONET measurements. *J. Atmos. Sci.* **2002**, *59*, 398–413. [CrossRef]
25. Torres, O.; Tanskanen, A.; Veihelmann, B.; Ahn, C.; Braak, R.; Bhartia, P.K.; Veefkind, P.; Levelt, P. Aerosols and surface UV products from ozone monitoring instrument observations: An overview. *J. Geophys. Res.* **2007**, *112*, D24S47. [CrossRef]
26. Vidot, J.; Santer, R.; Aznay, O. Evaluation of the meris aerosol product over land with AERONET. *Atmo. Chem. Phys.* **2008**, *8*, 7603–7617. [CrossRef]
27. Kaufman, Y.J.; Tanr, D.; Remer, L.A.; Vermote, E.F.; Chu, A. Operational remote sensing of tropospheric aerosol over land from EOS moderate resolution imaging spectroradiometer after the launch of MODIS the distribution. *J. Geophys. Res. Atmos.* **1997**, *102*, 17051–17067. [CrossRef]
28. Levy, R.C.; Remer, L.a.; Mattoo, S.; Vermote, E.F.; Kaufman, Y.J. Second-generation operational algorithm: Retrieval of aerosol properties over land from inversion of moderate resolution imaging spectroradiometer spectral reflectance. *J. Geophys. Res.* **2007**, *112*, D13211. [CrossRef]
29. Tanré, D.; Kaufman, Y.J.; Herman, M.; Mattoo, S. Remote sensing of aerosol properties over oceans using the MODIS/EOS spectral radiances. *J. Geophys. Res. Atmos.* **1997**, *102*, 16971–16988. [CrossRef]
30. Hsu, N.C.; Tsay, S.-C.; King, M.D.; Herman, J.R. Aerosol properties over bright-reflecting source regions. *IEEE Trans. Geosci. Remote Sens.* **2004**, *42*, 557–569. [CrossRef]
31. Hsu, N.C.; Tsay, S.-C.; King, M.D.; Herman, J.R. Deep blue retrievals of asian aerosol properties during ACE-Asia. *IEEE Trans. Geosci. Remote Sens.* **2006**, *44*, 3180–3195. [CrossRef]
32. Remer, L.A.; Mattoo, S.; Levy, R.C.; Munchak, L.A. MODIS 3 km aerosol product: Algorithm and global perspective. *Atmos. Meas. Tech.* **2013**, *6*, 1829–1844. [CrossRef]
33. Munchak, L.A.; Levy, R.C.; Mattoo, S.; Remer, L.A.; Holben, B.N.; Schafer, J.S.; Hostetler, C.A.; Ferrare, R.A. Modis 3 km aerosol product: Applications over land in an urban/suburban region. *Atmos. Meas. Tech.* **2013**, *6*, 1747–1759. [CrossRef]
34. Livingston, J.M.; Redemann, J.; Shinozuka, Y.; Johnson, R.; Russell, P.B.; Zhang, Q.; Mattoo, S.; Remer, L.; Levy, R.; Munchak, L.; et al. Comparison of MODIS 3 km and 10 km resolution aerosol optical depth retrievals over land with airborne sunphotometer measurements during arctas summer 2008. *Atmo. Chem. Phys.* **2014**, *14*, 2015–2038. [CrossRef]
35. Bilal, M.; Nichol, J.E. Evaluation of MODIS aerosol retrieval algorithms over the Beijing-Tianjin-Hebei region during low to very high pollution events. *J. Geophys. Res. Atmos.* **2015**, *120*, 7941–7957. [CrossRef]
36. Nichol, J.; Bilal, M. Validation of MODIS 3 km resolution aerosol optical depth retrievals over Asia. *Remote Sens.* **2016**, *8*, 328. [CrossRef]
37. Sayer, A.M.; Hsu, N.C.; Bettenhausen, C.; Jeong, M.-J. Validation and uncertainty estimates for MODIS Collection 6 "deep blue" aerosol data. *J. Geophys. Res. Atmos.* **2013**, *118*, 7864–7872. [CrossRef]
38. Sayer, A.M.; Munchak, L.A.; Hsu, N.C.; Levy, R.C.; Bettenhausen, C.; Jeong, M.J. MODIS Collection 6 aerosol products: Comparison between Aqua's e-deep blue, dark target, and "merged" data sets, and usage recommendations. *J. Geophys. Res. Atmos.* **2014**, *119*, 13965–13989. [CrossRef]
39. Bilal, M.; Nichol, J.; Wang, L. New customized methods for improvement of the MODIS C6 dark target and deep blue merged aerosol product. *Remote Sens. Environ.* **2017**, *197*, 115–124. [CrossRef]
40. Tao, M.; Chen, L.; Wang, Z.; Tao, J.; Che, H.; Wang, X.; Wang, Y. Comparison and evaluation of the MODIS Collection 6 aerosol data in China. *J. Geophys. Res. Atmos.* **2015**, *120*, 6992–7005. [CrossRef]
41. Mhawish, A.; Banerjee, T.; Broday, D.M.; Misra, A.; Tripathi, S.N. Evaluation of MODIS Collection 6 aerosol retrieval algorithms over indo-gangetic plain: Implications of aerosols types and mass loading. *Remote Sens. Environ.* **2017**, *201*, 297–313. [CrossRef]

42. Bilal, M.; Nazeer, M.; Nichol, J.E. Validation of MODIS and VIIRS derived aerosol optical depth over complex coastal waters. *Atmos. Res.* **2017**, *186*, 43–50. [CrossRef]
43. Bilal, M.; Nichol, J.E.; Chan, P.W. Validation and accuracy assessment of a simplified aerosol retrieval algorithm (sara) over Beijing under low and high aerosol loadings and dust storms. *Remote Sens. Environ.* **2014**, *153*, 50–60. [CrossRef]
44. Bilal, M.; Nichol, J.E.; Bleiweiss, M.P.; Dubois, D. A simplified high resolution MODIS aerosol retrieval algorithm (sara) for use over mixed surfaces. *Remote Sens. Environ.* **2013**, *136*, 135–145. [CrossRef]
45. Sun, L.; Wei, J.; Bilal, M.; Tian, X.; Jia, C.; Guo, Y.; Mi, X. Aerosol optical depth retrieval over bright areas using landsat 8 oli images. *Remote Sens.* **2016**, *8*, 23. [CrossRef]
46. Mateos, D.; Bilbao, J.; Kudish, A.I.; Parisi, A.V.; Carbajal, G.; di Sarra, A.; Román, R.; de Miguel, A. Validation of omi satellite erythemal daily dose retrievals using ground-based measurements from fourteen stations. *Remote Sens. Environ.* **2013**, *128*, 1–10. [CrossRef]
47. Bilal, M.; Nichol, J. Evaluation of the NDVI-based pixel selection criteria of the MODIS C6 dark target and deep blue combined aerosol product. *IEEE J. Sel. Top. Appl. Earth Obs. Remote Sens.* **2017**, *10*, 3448–3453. [CrossRef]
48. He, L.; Wang, L.; Lin, A.; Zhang, M.; Bilal, M.; Wei, J. Performance of the NPP-VIIRS and Aqua-MODIS aerosol optical depth products over the Yangtze River Basin. *Remote Sens.* **2018**, *10*, 117. [CrossRef]
49. Wei, J.; Sun, L.; Huang, B.; Bilal, M.; Zhang, Z.; Wang, L. Verification, improvement and application of aerosol optical depths in China part 1: Inter-comparison of NPP-VIIRS and Aqua-MODIS. *Atmos. Environ.* **2018**, *175*, 221–233. [CrossRef]
50. Sayer, A.M.; Hsu, N.C.; Bettenhausen, C.; Jeong, M.J.; Meister, G. Effect of MODIS terra radiometric calibration improvements on Collection 6 deep blue aerosol products: Validation and Terra/Aqua consistency. *J. Geophys. Res. Atmos.* **2015**, *120*, 12157–12174. [CrossRef]
51. Bilal, M.; Nichol, J.; Spak, S. A new approach for estimation of fine particulate concentrations using satellite aerosol optical depth and binning of meteorological variables. *Aerosol Air Qual. Res.* **2017**, *11*, 356–367. [CrossRef]
52. Zou, B.; Pu, Q.; Bilal, M.; Weng, Q.; Zhai, L.; Nichol, J.E. High-resolution satellite mapping of fine particulates based on geographically weighted regression. *IEEE Geosci. Remote Sens. Lett.* **2016**, *13*, 495–499. [CrossRef]
53. You, W.; Zang, Z.; Zhang, L.; Li, Y.; Wang, W. Estimating national-scale ground-level PM25 concentration in China using geographically weighted regression based on MODIS and MISR AOD. *Environ. Sci. Pollut. Res. Int.* **2016**, *23*, 8327–8338. [CrossRef] [PubMed]
54. Li, R.; Gong, J.; Chen, L.; Wang, Z. Estimating ground-level PM2.5 using fine-resolution satellite data in the megacity of Beijing, China. *Aerosol Air Qual. Res.* **2015**, *15*, 1347–1356. [CrossRef]
55. Ma, Z.; Hu, X.; Sayer, A.M.; Levy, R.; Zhang, Q.; Xue, Y.; Tong, S.; Bi, J.; Huang, L.; Liu, Y. Satellite-based spatiotemporal trends in PM2.5 concentrations: China, 2004–2013. *Environ. Health Perspect.* **2015**, *124*, 184–192. [CrossRef] [PubMed]
56. Geng, G.; Zhang, Q.; Marin, R.V.; Donkelaar, A.V.; Huo, H.; Che, H.; Lin, J.; He, K. Estimating long-term PM2.5 concentrations in China using satellite-based aerosol optical depth and a chemical transport model. *Remote Sens. Environ.* **2015**, *166*, 262–270. [CrossRef]
57. Guo, Y.; Feng, N.; Christopher, S.A.; Kang, P.; Zhan, F.B.; Hong, S. Satellite remote sensing of fine particulate matter ($PM_{2.5}$) air quality over Beijing using MODIS. *Int. J. Remote Sens.* **2014**, *35*, 6522–6544. [CrossRef]
58. Ma, Z.; Hu, X.; Huang, L.; Bi, J.; Liu, Y. Estimating ground-level PM2.5 in China using satellite remote sensing. *Environ. Sci. Technol.* **2014**, *48*, 7436–7444. [CrossRef] [PubMed]
59. Snider, G.; Weagle, C.L.; Martin, R.V.; van Donkelaar, A.; Conrad, K.; Cunningham, D.; Gordon, C.; Zwicker, M.; Akoshile, C.; Artaxo, P.; et al. Spartan: A global network to evaluate and enhance satellite-based estimates of ground-level particulate matter for global health applications. *Atmos. Meas. Tech. Discuss* **2014**, *7*, 7569–7611. [CrossRef]
60. Saunders, R.O.; Kahl, J.D.W.; Ghorai, J.K. Improved estimation of PM2.5 using lagrangian satellite-measured aerosol optical depth. *Atmos. Environ.* **2014**, *91*, 146–153. [CrossRef]
61. Toth, T.D.; Zhang, J.; Campbell, J.R.; Hyer, E.J.; Reid, J.S.; Shi, Y.; Westphal, D.L. Impact of data quality and surface-to-column representativeness on the $PM_{2.5}$/satellite AOD relationship for the contiguous United States. *Atmos. Chem. Phys.* **2014**, *14*, 6049–6062. [CrossRef]

62. Fang, X.; Zou, B.; Liu, X.; Sternberg, T.; Zhai, L. Satellite-based ground PM2.5 estimation using timely structure adaptive modeling. *Remote Sens. Environ.* **2017**, *186*, 152–163. [CrossRef]
63. Zou, B.; Wang, M.; Wan, N.; Wilson, J.G.; Fang, X.; Tang, Y. Spatial modeling of PM2.5 concentrations with a multifactoral radial basis function neural network. *Environ. Sci. Pollut. Res. Int.* **2015**, *22*, 10395–10404. [CrossRef] [PubMed]
64. Zou, B.; Luo, Y.; Wan, N.; Zheng, Z.; Sternberg, T.; Liao, Y. Performance comparison of LUR and OK in PM2.5 concentration mapping: A multidimensional perspective. *Sci. Rep.* **2015**, *5*, 8698. [CrossRef] [PubMed]
65. Parker, J.A.; Kenyon, R.V.; Troxel, D.E. Comparison of interpolating methods for image resampling. *IEEE Trans. Med. Imaging* **1983**, *2*, 31–39. [CrossRef] [PubMed]
66. Lehmann, T.M.; Gonner, C.; Spitzer, K. Survey: Interpolation methods in medical image processing. *IEEE Trans. Med. Imaging* **1999**, *18*, 1049–1075. [CrossRef] [PubMed]
67. Remer, L.A.; Kleidman, R.G.; Levy, R.C.; Kaufman, Y.J.; Tanré, D.; Mattoo, S.; Martins, J.V.; Ichoku, C.; Koren, I.; Yu, H.; et al. Global aerosol climatology from the MODIS satellite sensors. *J. Geophys. Res.* **2008**, *113*, D14S07. [CrossRef]
68. Bilal, M.; Nichol, J.E.; Nazeer, M. Validation of Aqua-MODIS C051 and C006 operational aerosol products using AERONET measurements over Pakistan. *IEEE J. Sel. Top. Appl. Earth Obs. Remote Sens.* **2016**, *9*, 2074–2080. [CrossRef]
69. Ichoku, C.; Remer, L.A.; Kaufman, Y.J.; Levy, R.C.; Chu, D.A.; Tanré, D.; Holben, B.N. Modis observation of aerosols and estimation of aerosol radiative forcing over Southern Africa during SAFARI 2000. *J. Geophys. Res.* **2003**, *108*, 8499. [CrossRef]